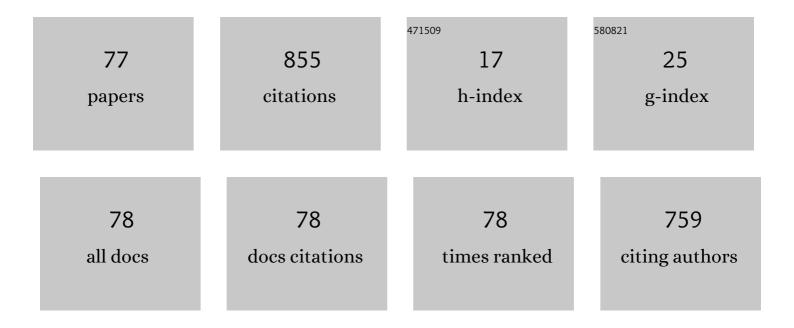
Kiyoshi Kobayashi

List of Publications by Year in descending order

Source: https://exaly.com/author-pdf/2224135/publications.pdf Version: 2024-02-01



#	Article	IF	CITATIONS
1	Structural study and proton transport of bulk nanograined Y-doped BaZrO3 oxide protonics materials. Solid State Ionics, 2008, 179, 236-242.	2.7	99
2	Electronic transport properties and electronic structure of InO1.5-doped CaZrO3. Solid State Ionics, 2000, 136-137, 305-311.	2.7	52
3	Structural changes of a Pd-based membrane during direct hydroxylation of benzene to phenol. Catalysis Today, 2006, 118, 57-62.	4.4	34
4	Calculation of the density of states of transition metal monosilicides by a first-principle pseudopotential method using plane-wave basis. Intermetallics, 2001, 9, 261-268.	3.9	33
5	Water-based sol–gel synthesis and crystal structure refinement of lanthanum silicate apatite. Solid State Ionics, 2008, 179, 2209-2215.	2.7	27
6	Sol–gel synthesis and ionic conductivity of oxyapatite-type La9.33+xSi6O26+1.5x. Journal of Power Sources, 2013, 235, 62-66.	7.8	27
7	Electronic transport properties and electronic structure of TiO2-doped YSZ. Solid State Ionics, 2000, 135, 643-651.	2.7	25
8	Photoemission Study on Protonic Conductor CaZrO3: Evidence of the Exchange Mechanism of Proton and Hole. Japanese Journal of Applied Physics, 2000, 39, L133-L136.	1.5	25
9	Proton incorporation and defect chemistry of Yb-doped BaPrO3. Solid State Ionics, 2007, 178, 641-647.	2.7	25
10	Research progress in nondoped lanthanoid silicate oxyapatites as new oxygen-ion conductors. Journal of the Ceramic Society of Japan, 2014, 122, 921-939.	1.1	25
11	Oxygen permeation and electrical transport properties of 60 vol.% Bi1.6Y0.4O3 and 40 vol.% Ag composite prepared by the sol?gel method. Solid State Ionics, 2004, 175, 405-408.	2.7	24
12	Thermoelectric properties and defect structure of La0.45Nd0.45Sr0.1FeO3âÂ^'δ. Solid State Ionics, 2001, 144, 123-132.	2.7	23
13	Powder neutron diffraction of La-apatite under low temperature. Nuclear Instruments and Methods in Physics Research, Section A: Accelerators, Spectrometers, Detectors and Associated Equipment, 2009, 600, 319-321.	1.6	23
14	Rudimental research progress of rare-earth silicate oxyapatites: their identification as a new compound until discovery of their oxygen ion conductivity. Journal of the Ceramic Society of Japan, 2014, 122, 649-663.	1.1	22
15	Fabrication of GDC/LSGM/GDC tri-layers on polypyrrole-coated NiO-YSZ by electrophoretic deposition for anode-supported SOFC. Journal of the Ceramic Society of Japan, 2009, 117, 1246-1248.	1.1	20
16	Distribution of Relaxation Time Analysis for Non-ideal Immittance Spectrum: Discussion and Progress. Journal of the Physical Society of Japan, 2018, 87, 094002.	1.6	19
17	Development of an electrochemical impedance analysis program based on the expanded measurement model. Journal of the Ceramic Society of Japan, 2016, 124, 943-949.	1.1	18
18	Transition metal-doped lanthanum germanate apatites as electrolyte materials of solid oxide fuel cells. Solid State Ionics, 2013, 247-248, 48-55.	2.7	17

#	Article	IF	CITATIONS
19	Phase Relation of ZrO ₂ -YO _{1.5} -TiO ₂ Ceramics Prepared by Sol-Gel Method. Journal of the Ceramic Society of Japan, 1998, 106, 860-866.	1.3	13
20	Development of Impedance Analysis Software Implementing a Support Function to Find Good Initial Guess Using an Interactive Graphical User Interface. Electrochemistry, 2020, 88, 39-44.	1.4	13
21	Free Analysis and Visualization Programs for Electrochemical Impedance Spectroscopy Coded in Python. Electrochemistry, 2021, 89, 218-222.	1.4	13
22	Low-temperature formation of Ln silicate oxyapatite (Ln=La and Nd) by the water-based sol–gel method. Solid State Ionics, 2011, 204-205, 91-96.	2.7	12
23	Electronic Transport Properties ofZrTiO4at High Temperature. Japanese Journal of Applied Physics, 1994, 33, 5471-5476.	1.5	11
24	Electronic Structure in the Bulk State of Protonic Conductor CaZrO3 by Resonant Soft-X-Ray Emission Spectroscopy. Japanese Journal of Applied Physics, 2002, 41, L938-L940.	1.5	11
25	Ester Condensation from a Stoichiometric Mixture of a Carboxylic Acid and an Alcohol at 313 K Assisted by Pervaporation via Zeolite Membranes. Chemistry Letters, 2006, 35, 76-77.	1.3	10
26	Theoretical modeling of electrode impedance for an oxygen ion conductor and metallic electrode system based on the interfacial conductivity theory. Solid State Ionics, 2013, 232, 49-57.	2.7	10
27	Chemical Reactivity and Cathode Properties of LaCoO ₃ on Lanthanum Silicate Oxyapatite Electrolyte. Key Engineering Materials, 0, 616, 120-128.	0.4	10
28	The effect of local structure on ionic conductivity of apatite-type La9.5Si6O26.25. Journal of Power Sources, 2014, 248, 685-689.	7.8	10
29	Fabrication of BSCF-based mixed oxide ionic-electronic conducting multi-layered membrane by sequential electrophoretic deposition process. Journal of the European Ceramic Society, 2021, 41, 2709-2715.	5.7	10
30	Synthesis and oxygen permeation properties of 75Âmol% Ce0.75Nd0.25O1.875–25Âmol% Nd1.8Ce0.2CuO4 composite. Journal of Solid State Electrochemistry, 2006, 10, 629-634.	2.5	9
31	Electrical Transport and Electric Power Generation Properties of Lanthanum Silicate Oxyapatite Ceramics Prepared by a Sol-gel Method. ECS Transactions, 2009, 25, 1785-1790.	0.5	9
32	Fabrication of BSCF-based mixed ionic-electronic conducting membrane by electrophoretic deposition for oxygen separation application. Journal of the European Ceramic Society, 2019, 39, 5292-5297.	5.7	9
33	Cross-sectional Area Dependency of Shrinkages and Grain Sizes of Flash-sintered 3 mol%Y ₂ O ₃ –ZrO ₂ Polycrystals with a Circular Truncated Cone-shape at High Frequency Alternating Electric Current Fields. Funtai Oyobi Fummatsu Yakin/lournal of the Japan Society of Powder and Powder Metallurgy. 2021. 68. 487-493.	0.2	9
34	Extended Distribution of Relaxation Time Analysis for Electrochemical Impedance Spectroscopy. Electrochemistry, 2022, 90, 017004-017004.	1.4	9
35	Excess oxygen-vacancy formed by FAST regime of direct-current electric field during flash sintering for 3Âmol%–10Âmol% Y2O3-doped ZrO2. Ceramics International, 2022, 48, 12091-12097.	4.8	9
36	Metastable Phase Relationship in the ZrO ₂ -YO _{1.5} , ZrO ₂ -TiO ₂ and YO _{1.5} -TiO ₂ Systems. Journal of the Ceramic Society of Japan, 1998, 106, 782-786.	1.3	8

#	Article	IF	CITATIONS
37	Theoretical modeling of electrode impedance for an oxygen ion conductor and metallic electrode system based on the interfacial conductivity theory. Part II: Case of the limiting process by non-steady-state surface diffusion. Solid State Ionics, 2013, 249-250, 78-85.	2.7	8
38	Discovery of a new crystalline phase: BiGeO ₂ (OH) ₂ (NO ₃). CrystEngComm, 2014, 16, 10080-10088.	2.6	8
39	Sinterable powder fabrication of lanthanum silicate oxyapatite based on solid-state reaction method. Journal of the Ceramic Society of Japan, 2015, 123, 274-279.	1.1	8
40	Total Electrical Conductivity Measurements of TiO ₂ Doped YSZ Ceramics. Journal of the Ceramic Society of Japan, 1998, 106, 1073-1078.	1.3	7
41	Band Structure of TiO2-Doped Yttria-Stabilized Zirconia Probed by Soft-X-Ray Spectroscopy. Japanese Journal of Applied Physics, 2003, 42, L941-L943.	1.5	7
42	Phase relationships in the quasi-ternary LaO1.5–SiO2–MgO system at 1773 K. Science and Technology of Advanced Materials, 2012, 13, 045006.	6.1	7
43	Room-temperature synthesis of Bi ₄ Ge ₃ O ₁₂ from aqueous solution. Japanese Journal of Applied Physics, 2015, 54, 06FJ03.	1.5	7
44	Research and Development of the Coprecipitation Process for Lanthanum Germanate Oxyapatite. Journal of the American Ceramic Society, 2015, 98, 66-70.	3.8	6
45	Enhanced ionic conductivity of aluminum tungstate by crystallographic orientation in a strong magnetic field. Journal of the American Ceramic Society, 2021, 104, 6364.	3.8	6
46	Electrical conductivity and X-ray diffraction analysis of oxyapatite-type lanthanum silicate and neodymium silicate solid solution. Solid State Ionics, 2012, 225, 443-447.	2.7	5
47	Anisotropic Electric Conductivity and Battery Performance in <i>C</i> -axis Oriented Lanthanum Silicate Oxyapatite Prepared by Slip Casting in a Strong Magnetic Field. Materials Transactions, 2019, 60, 1949-1953.	1.2	5
48	Theoretical modelling of electrode overvoltage for an all-solid-state electrochemical device. Japanese Journal of Applied Physics, 2020, 59, SIIG04.	1.5	5
49	Magnesium ion distribution and defect concentrations of MgO-doped lanthanum silicate oxyapatite. Solid State Ionics, 2014, 258, 24-29.	2.7	4
50	Electrical properties of murataite modules with complex and large-volume fluorite-type superstructures. Materials Research Bulletin, 2016, 84, 254-258.	5.2	4
51	Highâ€pressure synthesis of a 12CaO·7Al ₂ O ₃ –12SrO·7Al ₂ O ₃ solid solution. Journal of the American Ceramic Society, 2017, 100, 1285-1289.	3.8	4
52	Development of an Algorithm for Automatic Analysis of the Impedance Spectrum Based on a Measurement Model. Journal of the Physical Society of Japan, 2018, 87, 034004.	1.6	4
53	Thermoelectric Properties, Defect Structure, and Electronic Structure of Ln _{0.9} Sr _{0.1} FeO _{3â^'} <i>_δ</i> (Ln = La and Nd). Electrochemistry, 2004, 72, 870-875.	1.4	4
54	Electronic Structure of Ce1-xNdxO2-ÎProbed by Soft-X-Ray Spectroscopy. Japanese Journal of Applied Physics, 2004, 43, L1463-L1465.	1.5	3

#	Article	IF	CITATIONS
55	Preparation of palladium film by coating photolysis process using KrF or ArF excimer laser. Applied Surface Science, 2006, 252, 2858-2866.	6.1	3
56	Low-Tepmerature Synthesis Process of Lanthanum Germanate Oxyapatite by Citrate Combustion Method. Funtai Oyobi Fummatsu Yakin/Journal of the Japan Society of Powder and Powder Metallurgy, 2014, 61, 582-586.	0.2	3
57	Stabilization of the high-temperature phase and total conductivity of yttrium-doped lanthanum germanate oxyapatite. Journal of the Ceramic Society of Japan, 2018, 126, 91-98.	1.1	3
58	Production of crystal-oriented lanthanum silicate oxyapatite ceramics with anisotropic electrical conductivity and thermal expansion. Open Ceramics, 2021, 6, 100100.	2.0	3
59	Theoretical V–I characteristics of the solid-oxide thermocell using the oxide ion and electronic mixed conductors. Solid State Ionics, 2002, 154-155, 101-107.	2.7	2
60	Preparation of Porous Carbon Spheres Dispersed with Pd–Ag Alloy Nanoparticles. Chemistry Letters, 2007, 36, 152-153.	1.3	2
61	Electrophretic Deposition of LDC/LSGM/LDC Tri-layers on NiO-YSZ for Anode-supported SOFC. Transactions of the Materials Research Society of Japan, 2010, 35, 723-725.	0.2	2
62	Surface Structures and Electrochemical Activity of Palladium–Niobium Binary Alloy Electrodes, and Glucose Biosensor with Palladium–Niobium Binary Alloy Electrode. Bulletin of the Chemical Society of Japan, 2013, 86, 1317-1322.	3.2	2
63	Unconventional upright layer orientation and considerable enhancement of proton–electron conductivity in Dion–Jacobson perovskite thin films. CrystEngComm, 2014, 16, 4113-4119.	2.6	2
64	Growth of small GeO ₂ single crystals on a polyvinyl chloride substrate at room temperature using oversaturate aqueous solution. Electronics and Communications in Japan, 2019, 102, 12-16.	0.5	1
65	Electrode overvoltage model for a flash state of yttria-stabilized zirconia: validity, limitation, and open new issue. Journal of the Ceramic Society of Japan, 2022, 130, 172-179.	1.1	1
66	Anisotropic thermal expansion and ionic conductivity of a crystal-oriented, Mg2+-conducting NASICON-type solid electrolyte. Ceramics International, 2022, 48, 10733-10740.	4.8	1
67	Hydrogen Gas Diffusion Electrode Prepared from Porous Carbon Spheres Dispersed with Pd–Ag Alloy Nanoparticles. Bulletin of the Chemical Society of Japan, 2007, 80, 2243-2245.	3.2	0
68	Bulk-Nanograined BaScO2(OH) as a New Class of Oxide Protonics Materials. ECS Meeting Abstracts, 2008, , .	0.0	0
69	Surface morphological structures and electrochemical activity properties of iridium–niobium binary alloy electrodes. Materials Science and Engineering B: Solid-State Materials for Advanced Technology, 2013, 178, 1104-1109.	3.5	0
70	Surface Modification of Complex Oxide Powder with Polyelectrolyte Layers Improving EPD Characteristics. Key Engineering Materials, 0, 654, 255-260.	0.4	0
71	Anisotropic Electronic Conductivity and Battery Performance in C-axis Oriented Lanthanum Silicate Oxyapatite Prepared by Slip Casting in a Strong Magnetic Field. Funtai Oyobi Fummatsu Yakin/Journal of the Japan Society of Powder and Powder Metallurgy, 2018, 65, 121-126.	0.2	0
72	OXYGEN PERMEABILITY OF 60-VOLUME% Bi _{1.6} Y _{0.4} O ₃ AND 40-VOLUME% Ag COMPOSITE PREPARED BY CITRATE SOL-GEL METHOD. , 2002, , .		0

#	Article	IF	CITATIONS
73	Sinterable Powder Fabrication and the Oxygen-ion Conductivity of Lanthanum Silicate Oxyapatite. Journal of the Society of Powder Technology, Japan, 2015, 52, 648-657.	0.1	Ο
74	Growth of Small GeO ₂ Single Crystals on a Polyvinyl Chloride Substrate at Room Temperature using Oversaturate Aqueous Solution. IEEJ Transactions on Electronics, Information and Systems, 2019, 139, 203-206.	0.2	0
75	pH-controlled synthesis and spark plasma sintering of fine and homogeneous MgZr ₄ (PO ₄) ₆ powder. Journal of the Ceramic Society of Japan, 2022, 130, 243-248.	1.1	Ο
76	Synchronization Phenomena Originating from Quantum Effects of Photon Fields. Journal of the Physical Society of Japan, 2022, 91, .	1.6	0
77	Theory of Electrode Overvoltage for Stabilized Zirconia Solid Electrolyte and Its Application to Several Topics. Materia Japan, 2022, 61, 210-217.	0.1	0